HHS Public Access

Author manuscript

*Neurogastroenterol Motil*. Author manuscript; available in PMC 2024 August 05.

Published in final edited form as:

*Neurogastroenterol Motil*. 2023 November ; 35(11): e14646. doi:10.1111/nmo.14646.

# Plasticity of colonic enteric nervous system following spinal cord injury in male and female rats

**Claire M. Werner**,
**Lisa B. Willing**,
**Hannah J. Goudsward**,
**Amanda R. McBride**,
**Salvatore L. Stella Jr**,
**Gregory M. Holmes**

Department of Neural and Behavioral Sciences, Penn State University College of Medicine, Hershey, Pennsylvania, USA

## Abstract

**Background:** Neurogenic bowel is a dysmotility disorder following spinal cord injury (SCI) that negatively impacts quality of life, social integration, and physical health. Colonic transit is directly modulated by the enteric nervous system. Interstitial Cells of Cajal (ICC) distributed throughout the small intestine and colon serve as specialized pacemaker cells, generating rhythmic electrical slow waves within intestinal smooth muscle, or serve as an interface between smooth muscle cells and enteric motor neurons of the myenteric plexus. Interstitial Cells of Cajal loss has been reported for other preclinical models of dysmotility, and our previous experimental SCI study provided evidence of reduced excitatory and inhibitory enteric neuronal count and smooth muscle neural control.

**Methods:** Immunohistochemistry for the ICC-specific marker c-Kit was utilized to examine neuromuscular remodeling of the distal colon in male and female rats with experimental SCI.

**Key Results:** Myenteric plexus ICC (ICC-MP) exhibited increased cell counts 3 days following SCI in male rats, but did not significantly increase in females until 3 weeks after SCI. On average, ICC-MP total primary arborization length increased significantly in male rats at 3-day, 3-week, and 6-week time points, whereas in females, this increase occurred most frequently at 6 weeks post-SCI. Conversely, circular muscle ICC (ICC-CM) did not demonstrate post-SCI changes.



**Correspondence**: Gregory M. Holmes, Department of Neural and Behavioral Sciences, Penn State University College of Medicine, 500 University Dr., H109, Hershey, PA 17033, USA. gmh16@psu.edu.

AUTHOR CONTRIBUTIONS

CMW and GMH designed the experiments. CMW, LBW, and SLS, Jr. were involved in ICC, confocal microscopy collection and interpretation. CMW and HJG performed histology and brightfield microscopy analysis. CMW and GMH were involved in the interpretation of data. CMW, SLS, Jr., and GMH drafted the manuscript. All authors read, edited, and approved the final version of manuscript.

CONFLICT OF INTEREST STATEMENT

No competing interests declared.

**Conclusions and Inferences:** These data demonstrate resiliency of the ICC-MP in neurogenic bowel following SCI, unlike seen in other related disease states. This plasticity underscores the need to further understand neuromuscular changes driving colonic dysmotility after SCI in order to advance therapeutic targets for neurogenic bowel treatment.

**Keywords**

gastrointestinal motility; myenteric plexus; neurogenic bowel; spinal cord injuries

## 1 | INTRODUCTION

Spinal cord injury (SCI) is a devastating chronic disorder that results in widespread, multi-organ system dysfunction. Aside from decreased sensorimotor function, SCI frequently results in autonomic nervous system (ANS) dysregulation, such as gastrointestinal (GI) tract dysfunction, of which neurogenic bowel (NB) is the most common comorbidity. In individuals with SCI, NB is associated with symptoms such as constipation, overflow fecal incontinence, hemorrhoids, and disruptions in evacuation. Bowel-related symptoms greatly diminish quality of life and are therefore rated by individuals with SCI as high treatment priorities in physical and psychological capacities.[1–3] Presentation frequency of GI symptoms vary from 27% to 62%, and subsequent complications can vary from minor to severe symptoms, including hospitalization.[4] Therapeutic interventions and life-management strategies for NB are often anecdotal and suboptimal, reflecting fundamental knowledge gaps in the postinjury remodeling of the colonic ANS.

The enteric nervous system (ENS) provides quasi-autonomous reflex propulsion of GI contents that are further under the control of extrinsic innervation to achieve the homeostatic regulation of the GI tract. The wall of the distal colon has an outer longitudinal muscle and an inner circular muscle, which are separated by an intrinsic neural network known as the myenteric plexus. A key component of this neuromuscular interface is provided by Interstitial Cells of Cajal (ICC), which interface between smooth muscle cells and enteric neurons.[5,6] Throughout the GI tract, ICC consist of several heterogeneous subtypes that can be segregated by their morphology, location, and extent of electrical coupling through gap junctions with smooth muscle cells.[5,7] The myenteric plexus ICC (ICC-MP or ICC-MY) largely drive propulsive functions along the GI tract with the intramuscular ICC of the longitudinal (ICC-LM) and circular (ICC-CM) smooth muscle, whereas other ICC of the submucosal plexus potentiate vascular and secretory function.[6,8,9] During the peristaltic reflex, primary afferent neurons within the GI wall respond to chemical and mechanical GI changes, activating proximal (ascending) excitatory and distal (descending) inhibitory enteric neurons comprising the circuitry required to propel luminal contents.[10]

Interstitial Cells of Cajal express the receptor tyrosine kinase (c-Kit) and application of c-Kit antibody permits anatomical identification of ICC for functional studies of physiological regulation of gastrointestinal smooth muscle cells.[11] The ICC distributed within the ICC-MP as well as both intramuscular subtypes[12] generate slow-wave smooth muscle activity through ANO1 $Ca^{2+}$-activated chloride channels.[13] This interface drives smooth muscle

slow-wave activity by phasic calcium release, while simultaneously being under the influence of excitatory (ACh) and inhibitory (NO, ATP) neural inputs from the ENS.

Our previous work demonstrated that following experimental T3-SCI in male Wistar rats, the distal colon undergoes changes to the neuromuscular compartment comparable to human bowel diseases.[14] These changes include increased collagen, thickening of the smooth muscle, and neuronal cell loss within the myenteric plexus.[15] These anatomical changes were accompanied by reduced in vivo distal colon contractions.[15] We subsequently demonstrated reduced excitatory (cholinergic, ACh) and inhibitory (nitrergic, NO) neuromuscular transmission ex-vivo, at the enteric neuromuscular interface.[16] Collectively, the data indicate pathophysiological remodeling to the final common neural pathway to smooth muscle responsible for colonic transit.

In this study, we used male and female rats with T3-SCI or laminectomy-only control surgery to quantify ICC-MP and ICC-CM at 3-days, 3-weeks, and 6-weeks following surgery. Our results demonstrate that ICC-MP undergo post-SCI expansion in both cell number and the extent of primary arborizations, whereas no changes are seen in the ICC-CM. We propose that cell loss within the colonic neuromuscular compartment may provoke remodeling of ICC-MP following SCI.

## 2 | MATERIALS AND METHODS

### 2.1 | Experimental groups and objectives

The principal objective of this study was to quantify the impact of severe, high-thoracic SCI on the ICC distribution and morphology of the distal colon ICC-MP and ICC-CM. All rats were randomly assigned to receive a surgical control (T2 laminectomy) or T3 spinal segment contusion SCI ($n$ = 32 males, $n$ = 34 females). This level of injury is most translational to the human population of injuries and additionally, this injury disrupts all sympathetic innervation to the colon. Postoperatively, animals were further divided into an acute 3-day, stabilizing 3-week, or chronic 6-week time point; this variable will be referred to as “duration” following surgery. There was a minimum of five animals per group.

### 2.2 | Animals

Male and female Wistar rats entered experimentation between 6 and 8 weeks of age (Hsd:WI, Stock 001; Envigo). Rats arrived weighing 150–174 g and were housed two to a cage with food and water ad libitum. Following surgical intervention, rats were singly housed. They were maintained at 21–24°C, with a 12:12-h light–dark cycle. All animal research procedures followed the National Institute of Health guidelines and were approved by the Penn State College of Medicine Institutional Animal Care and Use Committee.

### 2.3 | Surgical procedures and care

Prior to surgical procedures, animals were administered deep 3%–5% Isoflurane and oxygen (1 L/min) anesthesia, maintained at 35.5–37.5°C on a heating pad, and received ophthalmic ointment. Based on weight, they were administered subcutaneous (s.c.) Buprenorphine Slow Release (1 mg/kg; Reckitt Benckiser Pharmaceuticals Inc.) for post-operative pain and

Enroflox antibiotic (10 mg/mL concentration at 1 mL/kg; Bayer), and a local anesthetic cocktail consisting of a 1:1 preparation of Lidocaine/Bupivacaine (Lidocaine Hydrochloride inj 2%; Vedco Inc. and Bupivacaine HCl inj 0.25%; Hospira Inc.) at the incision site. The T1 spinous process was palpated and an incision was made extending from T1 to T3 after being shaved and cleaned twice with Chlorhexidine Acetate (Fort Dodge Animal Health) and 70% ethanol. The underlying musculature was cleared with blunt dissection to reveal the T1–T3 spinous processes and vertebral laminae. Using fine tipped rongeurs, a T2 laminectomy was conducted to expose the T3 spinal level.

Following laminectomy, only rats randomly selected for SCI were placed in the Infinite Horizon controlled impact device (Precision Systems and Instrumentation, LLC). For SCI rats, the T1 and T3 vertebrae were clamped, after which the spinal cord and overlying dura mater was hit with a rapid 300 kdyn force for a 15-s dwell time. At the conclusion of surgery, all rat's musculature was sutured with polyglactin and overlying skin was closed with 9 mm wound clips. Rats were then administered 5 mL s.c. of lactated Ringer's solution and placed in a 37°C incubation chamber for recovery until anesthesia subsided.

Following surgery, all animals were singly housed for the purpose of food intake measurements, with SCI animal cages placed on a warming unit (Gaymar T-pump; Stryker) to maintain body temperature. Rats were provided enrichment tubes or enclosures depending upon size and mobility. Postoperatively, all animals received s.c. Enroflox antibiotic once daily for 5 days and wound clips were removed after 5–7 days. SCI rats received supplemental fluids (5–10 mL b.i.d.) and manual compression of the bladder was performed until spontaneous voiding returned. To facilitate ease of access, SCI rats were provided chow in their bedding, and caloric intake and body weight were monitored daily in all animal groups to access overall well-being.

### 2.4 | Spinal cord harvest and histological processing

Upon euthanasia, the vertebrae and spinal cord at the level of SCI lesion or control surgery were harvested *en bloc* and postfixed in 4% paraformaldehyde. Following fixation, the spinal cord was extracted and embedded in OCT to be cryosectioned at 40 μm to confirm the extent of T3 lesion. Transverse cross-sections were mounted on gelatin-coated slides and stained with Luxol Fast Blue (LFB) to visualize spared, myelinated fibers. The slides were digitally imaged on a Zeiss Axioscope light microscope and Axiocam CCD camera, where they were imported into Adobe Photoshop. To determine percent white matter spared, spinal cord tissue boundaries were outlined to determine total cross-section area. Next, a threshold histogram was utilized to identify the pixels corresponding to LFB staining and quantified. LFB-stained myelin in injured tissue is represented as percent of total spinal cord cross-sectional area.

To confirm completeness of the injury, animals sacrificed 3 days postoperatively were considered a severe T3-SCI when ≤25% LFB-stained white matter remained in cross-section, while those presenting with >25% LFB-stained white matter were excluded from the study as previously described.[17,18] In the days following injury, the remaining myelinated fibers are due to myelin debris along with the small percentage of surviving myelinated fibers.[19] In contrast, animals euthanized postoperatively at the 3-or 6-week time

point are considered a severe T3-SCI when ≤5% LFB staining remains as myelin debris has been cleared and animals with lesion centers >5% were excluded from the study. After 3 weeks, any remaining LFB staining is usually confined to a thin band within the ventro-lateral white matter in a manner consistent with previous reports characterizing a 200 kdyn injury.[17] In all time points, animals classified as surgical controls must have ≥95% myelin sparing at T3 cross-sectional analysis.

### 2.5 | Distal colon harvest and immunohistochemistry

Immediately following euthanasia, an incision was made along the linea alba to expose the abdominopelvic cavity. A segment of the distal colon (~1 cm long) was extracted and placed in ice cold oxygenated Krebs solution as previously described.[16] The extracted colon was placed in a Sylgard lined petri dish and fresh Krebs solution was replaced every 15 min. The tissue was cut with microscissors along the mesenteric border to expose the lumen, stretched, and pinned taut. The mucosal and submucosal layers were bluntly dissected away with angled micro-forceps and separated from the smooth muscle layers. After the completion of dissection, the inner circular and outer longitudinal smooth muscle remained stretched and were fixed with 4% paraformaldehyde for at least 2–4 h (up to overnight) and then placed into 0.05% sodium Azide in 1× PBS for long term storage.

For indirect immunofluorescent labeling, free floating incubation of dissected distal colon smooth muscle (~$0.5^2$ cm) was rinsed (3×) with PBS (pH 7.4). Tissue was then blocked with Ultravision Protein Block (Thermo Sci TA-060-PBQ). A 24-h primary incubation with cKIT/CD117 (R&D Systems AF1356 Polyclonal Goat IgG) was utilized to fluorescently label the network of ICC at a 1:500 dilution at 4°C. The following day, tissue was rinsed (3×) with PBS before dark secondary incubation (Alexa Fluor 488: Invitrogen/LifeTech A11055 Donkey-anti-goat) 1:600 with 2%BSA/PBS for 2 h. Following three washes with 1× PBS, tissue was mounted with the serosal side facing downward onto gelatin subbed slides and 1.5 mm coverslips with Aqua Poly/Mount (Polysciences). To verify specificity of the secondary antibody, controls were prepared by omitting the primary antibody during the incubation.

### 2.6 | Confocal imaging and analysis

Images of c-Kit immunohistochemistry were acquired with a Nikon C2+ confocal head mounted to an Eclipse FN-1 microscope (Nikon Instruments) equipped with three laser line excitation (488, 543, and 633 nm), Nomarski contrast, and controlled by Nikon Elements software (ver. 4.3). Full tissue thickness z-stack images of two randomly selected regions of the ~$0.5^2$ cm tissue piece was acquired per animal with a Plan Apochromat 40×/1.30 Oil DIC objective. Most confocal images were acquired at an approximate optical thickness of 0.5 μm. To create a pseudo-3-dimensional relief of the sample, bright field differential interference contrast (DIC) images were simultaneously obtained with a corresponding objective-matched DIC analyzer (prism) using the 488 nm laser as the light source and were collected using the transmitted light/diascopic detector (C2-DUT) mounted between the halogen light source and the microscope.

The entire 40× field of view was subsequently analyzed with Fuji ImageJ, and the myenteric ganglion layer was identified with Alexa Flour 488 labeling by noting the transition in fiber direction between circular and perpendicularly-oriented longitudinal smooth muscle (Figure 1). This was then confirmed by DIC images. Five z-stack slices prior to and past the point of transition were compressed into a maximum projection z-stack to uniformly capture the myenteric plexus for analysis of ICC-MP. In a similar manner, ICC-CM were isolated for analysis by creating a maximum projection z-stack by compressing slices from the outer extent of the ICC-MP to the inner luminal extent of the tissue.

The following variables were quantified for ICC-MP and ICC-CM for each animal: (1) all visible cell bodies were counted for each 40× image; (2) primary ICC arborizations whose entire cell projections fell within the field of view were counted per cell and then primary arborizations were (3) measured using the plugin NeuronJ (semi-automated neuronal process tracer). Primary arborizations were defined as those arising directly from the cell body and therefore, no secondary or tertiary branches were analyzed. Primary arborization branches from the maximum projection images were confirmed by scrolling through individual z-stack slices to better visualize the 3-dimensional morphology. For each variable, quantifications were done for two z-stacks per experimental animal. For variables 1 and 2, values were averaged. For variable 3, projection lengths were converted to microns and added for each traced ICC, generating a total primary arborization length per cell.

### 2.7 | Preparation of figures

Line art was generated with Adobe Photoshop 2021 (Adobe Systems). Individual photomicrograph images were converted from the proprietary Nikon file format to tagged image file format (TIF) and opened with Photoshop to organize the layout and apply text.

### 2.8 | Statistical analysis

All statistical calculations were performed in the GraphPad Prism 9 software (San Diego, CA). Groups were compared by two-way ANOVA followed by Tukey's multiple comparisons test. Interaction $p$-values are two-way ANOVA results and asterisks are representative of multiple comparison values. Results are expressed as mean ± SEM with significance defined as $p < 0.05$. All data were assessed for outliers using a Grubbs test macro written in GraphPad. Four individual cells were identified as outliers for ICC-MP total primary arborization length (two male, two female cells) and were excluded. Additionally, one rat for male multipolar ICC-CM cell count and one individual cell from male ICC-CM total primary arborization length were identified as outliers, so they too were excluded from analysis.

## 3 | RESULTS

### 3.1 | Experimental rats were confirmed as surgical controls or complete T3-SCI

Based upon previously outlined criteria, the final number of male rats for each group were as follows: 3-day T3-SCI, $n = 5$; 3-day control, $n = 5$; 3-week T3-SCI, $n = 5$; 3-week control, $n = 5$; 6-week T3-SCI, $n = 6$; 6-week control, $n = 6$. The cohort of female rats utilized were: 3-day T3-SCI, $n = 5$; 3-day control, $n = 5$; 3-week T3-SCI, $n = 7$; 3-week control, $n = 5$;

6-week T3-SCI, $n = 6$; 6-week control, $n = 6$. Following lesion analysis, all criteria was met and no animals were excluded from the study.

### 3.2 | Distal colon ICC-MP cell body counts increase after T3-SCI

Maximum projection visualization of the full thickness distal colon smooth muscle for c-Kit immunohistochemistry revealed a qualitative increase of overall ICC network in male (Figure 2) and female (Figure 3) rats following SCI. Upon quantification of cell bodies of the ICC-MP (all multipolar), two-way ANOVA revealed that both sexes have significant surgical model relationships ($P_{Surgery}$ Male < 0.0001, Female 0.0003) and females have a significant interaction value between duration and surgery ($P_{int} = 0.0005$). Tukey post hoc analysis revealed that on average, male rats show a significant increase in cell body count at 3-day ($p = 0.04$), 3-week ($p < 0.0001$), and 6-week ($p < 0.05$) time points following SCI (Figure 4A). There was no significant difference between any surgical control groups. The female rats on average demonstrated a significant increase in cell body count from 3-week surgical control to 3-week SCI ($p < 0.0001$), with no significant change between control groups (Figure 4B). Additionally, there was an observed significant increase in cell counts from 3-day to 3-week SCIs ($p = 0.0007$). Increases in ICC-MP cell counts were most notable at the 3-week time point for both male and female rats. These qualitative and quantitative results are indicative of significant ICC-MP proliferation following SCI. Also notable, there are different trends seen between sexes. Generally, females present with delayed ICC-MP cell body increases compared to corresponding male rats.

### 3.3 | Distal colon number of projections per ICC-MP remain unchanged after T3-SCI

The number of primary (cytoplasmic) projections arising directly from the soma of each cell body were counted. Following SCI, there is no significant change in the number of primary projections arising from ICC-MP cell bodies in either male (Figure 5A) or female groups (Figure 5B). In fact, the number of primary projections were conserved when compared across all animal groups, with the average number of ICC-MP projections arising from individual cell bodies ranging from 3.14 to 3.64 projections. These data suggest that despite the increased number of ICC-MP following SCI, cell bodies do not generate additional cytoplasmic projections contributing to ICC-MP plasticity.

### 3.4 | Distal colon ICC-MP total primary arborizations increase after T3-SCI

The length of total primary arborizations were quantified for individual ICC-MP cells. A total of 379 cell primary arborizations lengths were recorded, of which 194 were male and 185 were female. Two male and two female ICC-MP individual cell total arborization lengths were identified as outliers and were excluded from analysis. In male rats, on average, there was a significant increase in primary arborizations following SCI at the 3-day ($p < 0.0001$), 3-week ($p < 0.0001$), and 6-week ($p = 0.02$) time point (Figure 6A). In contrast to males, on average, the female rats displayed no significant increase in primary arborization following SCI until the 3-week ($p = 0.02$) and 6-week time points ($p = 0.0001$) (Figure 6B). These results demonstrate sex differences similar to the ICC-MP cell body counts, with females trending to have delayed lengthening of primary arborizations compared to males. Please note that on average, primary arborization lengths are increasing following SCI for both sexes, but this does not hold true for every single cell documented for a given animal.

### 3.5 | Distal colon ICC-CM cell body counts and primary arborizations remain unchanged after T3-SCI

The ICC within the circular smooth muscle fibers form a heterogeneous subtype that differ in morphology. The cell bodies of the ICC-CM were counted in male and female rats using the same criteria employed for ICC-MP cells. Measurements were performed independently for bipolar and multipolar ICC-CM due to known differences in their presentation frequency. One animal outlier was excluded from male multipolar cell count analysis. The majority of intramuscular ICC in male and female rats were identified as bipolar (72%), with a smaller population of multipolar cells (28%) (Figure 7). There were no significant differences in cell body counts across any groups. There was, however, a significant effect of time following surgery on male bipolar cell counts ($P_{Duration} = 0.01$).

In the ICC-CM, total primary arborization lengths per cell displayed no significant differences based on cell morphology and therefore total arborization cannot be used to differentiate between cell types (Figure 8). A total of 181 cell primary arborizations lengths were recorded, of which 80 were male and 101 were female. One individual cell was found to be an outlier among male primary arborization length and was excluded from analysis. Unlike the ICC-MP, there was no significant effect of time point or surgical model on ICC-CM primary arborization length in males or females.

## 4 | DISCUSSION

Our study explored the hypothesis that NB following T3-SCI is accompanied by extensive depletion and/or remodeling of the distal colon ICC networks, reminiscent of the loss of enteric neurons we previously reported.[15,16] The net depletion of ICC is widely recognized to occur in GI motility disorders and has received considerable attention.[20–23] However, no studies up to this point have investigated if this depletion occurs following SCI. The results of this study revealed a time-dependent increase in ICC-MP cell number and primary arborizations lengths following T3-SCI. Furthermore, we found that female rats consistently demonstrate a slower rate of post-SCI ICC-MP proliferation compared to males. Interestingly, the ICC network expansion was not observed for the ICC-CM in male or female rats.

### 4.1 | Potential mechanisms of ICC-MP proliferation and increased primary arborization

The mechanisms underlying the localized maintenance and remodeling of the enteric neuromuscular junction are not fully understood. One potential explanation for our observed increase in ICC-MP and their associated primary arborizations relates to the renewal process of these cells. Like the ENS,[24] ICC in the healthy gut undergo considerable self-renewal through a tightly controlled process of regeneration and depletion.[25] It is important to note that the development and preservation of ICC is dependent upon activation of c-Kit.[26–30] The ligand for c-Kit is stem cell factor (SCF), and SCF-deficient mice demonstrate loss of development and function in ICC-MP,[28,31] while other ICC populations do not display such deficits.[32] A previous study explored SCF and a complementary hematopoietic cytokine, granulocyte colony-stimulating factor (G-SCF), for functional motor efficacy following SCI,[33] but GI gain of function was not addressed. Subsequent

studies[34] emphasize SCI functional recovery following G-CSF therapy that is mediated through anti-inflammatory and anti-apoptotic mechanisms. The therapeutic efficacy of these cytokines on GI neuromuscular integrity remains to be determined.

The neuroeffector nitric oxide (NO) is both cytotoxic and cyto-protective,[35] and may provide another potential explanation for our observed ICC-MP proliferation and increased primary arborizations. The cytotoxic effects of NO may be more a function of the duration of availability rather than the local concentration.[36] In addition to effects upon enteric inhibitory neuronal transmission, diminished NO or the neuronally derived enzyme, NO synthase (nNOS), is associated with a reduction of ICC.[37,38] Specifically, an in vivo reduction of NO in $nNOS^{-/-}$ mice was accompanied by a reduction of ICC-MP in the gastric body, whereas in vitro exposure of organotypic muscularis explants from the same $nNOS^{-/-}$ strain mice to a NO donor expanded ICC-MP volume.[37] Conversely, oxidative stress induced by NO impairs pacemaker function of murine ICC during inflammation through a mechanism of trans-differentiation rather than apoptotic ICC reduction.[39] Considering that much of the study of NO cytotoxicity and cytoprotection has utilized in vitro techniques and GI tissue other than the colon, further investigation of this molecule is warranted in the context of the multiple parallel aerobic pathways found in vivo as well as the heterogeneous distribution and physiology of ICC subtypes.

One additional explanation for our upregulated ICC-MP ties to serotonin, as it exhibits a dual-effect upon vagal and enteric neuro-physiology[40–44] and ICC proliferation. One study showed ICC activation by serotonin through the 5-hyroxytryptamine $(5\text{-HT})_{2B}$ receptor dose-dependently promoted ICC proliferation[45] using in vitro approaches, but they did not differentiate between regionally different subtypes of ICC. Conversely, the deletion of $5\text{-HT}_{2B}$ receptor reduces the density of ICC networks in vivo.[46] The gastrointestinal localization of the $5\text{-HT}_4$ receptor has been described using immunolabeling. Abundant $5\text{-HT}_4$-positive labeling was seen in ICC-MP of the proximal and distal colon, while ICC-CM at the submucosa junction was sparsely labeled.[47] Similarly, the co-localization of $5\text{-HT}_3$ receptor on ICC-MP has been reported for the rat ileum,[48] though in neither case has a role in ICC proliferation been analyzed.

In summary, the contributions of ICC to the coordinated reflex contraction of the GI tract are widely accepted.[5,6] Most of our understanding is derived from loss-of-function studies that report reduced ICC numbers,[49–52] though the complex interplay of ICC number and ion channel density on surviving ICC must be considered with regard to the functional relevance of such findings.[53] Modeling studies propose that network oscillations are resistant to some degree of ICC loss,[54] while other studies have identified diabetic gain-of-function accompanied by ICC expansion.[55] In this later study the signaling pathway contributing to ICC expansion was demonstrated to involve the actions of mitogen-activated protein kinase 1 (MAPK1) and MAPK3 upon a master transcription factor for ICCs.[55] However, this mechanism was only demonstrated through the use of isolated ICC-lineage cells and organotypic cultures exposed to hyperglycemia. Our in vivo model of SCI does not induce long-term hyperglycemia in rats fed a standard laboratory diet but only when fed a high fat diet.[56,57] Furthermore, only the responsiveness to a cholinergic agonist was explored and cell counts for cholinergic excitatory and nitrergic inhibitory enteric

neurons were not performed nor were evoked responses in the form of smooth muscle junction potentials. Our previous report of reduced cholinergic and nitrergic myenteric neuron populations in SCI rats would be consistent with a loss-of-function, despite the increase in ICC networks.[16] Electrophysiological recording of smooth muscle membrane potential in response to pharmacologically targeted ICC activation would begin to clarify our understanding of how these increased ICC-MP networks effect colonic function.

### 4.2 | Sex differences impacting the regulation of ICC

Numerous sex-related differences in GI physiology are recognized in clinical and preclinical models and females are known to have a higher prevalence of GI-related disorders overall.[58–60] Despite these known differences, the influence of sex on enteric nervous system anatomy and function has been inconsistently studied, or not clearly isolated in mixed-sex studies. Additionally, steroid hormone receptors have been identified throughout the GI tract, which may have effects independent of CNS neurons that are typically thought to govern GI reflexes.[61–63] Functionally, estrogen receptors and estrogen receptor ligands have been shown to be inhibitory to colonic motility through actions on both inhibitory nitrergic and excitatory cholinergic junction potentials.[62,64]

This present study demonstrates female rats have delayed ICC-MP cell proliferation and primary arborization following SCI compared to male rats. Estrogen has been suggested to serve a neuroprotective role following SCI,[65] with some studies reporting better neurologic recovery compared to males.[66] These reports are complicated by the occurrence of amenorrhea in roughly 50% of new female SCI cases,[67] thereby eliciting an uncontrolled temporary hypoestrogenic state. Regardless of injury level or extent, amenorrhea lasts approximately 8 months in humans,[68] where a female T8 SCI rat model revealed estrous cycle returned roughly 9 days[67] following injury.

A hypoestrogenic state has also shown to impact ICC plasticity in a menopausal rat model studying detrusor overactivity.[69] Within the bladder wall, ICC populations were shown to decrease following ovariectomy, but were restored to control levels upon estrogen (17 β-estradiol) treatment.[69] Another study, Bassotti et al.,[70] collected human rectal tissue from individuals (16 women, 1 man) suffering from chronic constipation, localizing estrogen and progesterone receptors, enteric neurons, enteric glial cells, and all ICC subtypes. Echoing our present study, they found that individuals with obstructed defecation had a significant increase in ICC-MP and no change in intramuscular ICC, accompanied by a loss of enteric glial cells. Similarly to White et al.,[16] the study suggested that this increase in ICC populations could be a compensatory response to lack of neuronal input.[70] There was also a significant reduction in estrogen receptor β in the chronic constipation group, suggesting further connections between estrogen and ICC plasticity. Collectively, these studies support our current findings of ICC-MP and primary arborization increase after SCI. They also demonstrate the significance of experimentally monitoring estrous cycle disruption and hormonal levels following SCI. Therefore, the role of sex hormones on ICC plasticity deserves further investigation.

### 4.3 | Shortcomings and limitations

The current understanding of ICC structure and function is derived heavily from studies of the gastric and small intestinal networks, leaving much to be further investigated. One of our study's primary limitations was the absence of tracking estrous cycle. The variability in estrous cycle disruption following SCI, along with our findings that ICC in females remodel at rates slower than rat estrous cycle length collectively suggests that estrous cycle did not affect our results. We were also unable to analyze the ICC-LM, as this layer is difficult to visualize with c-Kit immunohistochemistry given that longitudinal muscle is significantly thinner than circular and therefore few cells can be identified in this layer.

## 5 | CONCLUSION

In summary, our data reveal that experimental SCI provokes a pronounced level of ICC plasticity. Significant male and female distal colon ICC proliferation and increased primary arborization lengths are specific to the myenteric plexus, while the ICC-CM remain unaltered. Increased ICC-MP networks coupled with the reduction of excitatory and inhibitory enteric neuromuscular transmission[16] demonstrates significant dysfunction in the final common pathway that generates propulsive contractions in the distal colon. Identifying that not all GI insults lead to the loss of cells, but rather that the ICC can be remarkably resilient is a unique finding among GI-related disease states. Further investigation is warranted to determine the point of dysregulation that results in functionally compromised bowel reflexes and motility after SCI. Consideration of the implications of this remodeling is essential for future application or development of therapeutic interventions for NB following SCI.

## ACKNOWLEDGMENTS

The authors wish to extend their gratitude for the support across multiple capacities and the input provided by Jackson B. Radler, and Gina Marcucci.

### FUNDING INFORMATION

This work was supported by National Institute of Neurological Disorders and Stroke (NINDS) Grant R01-NS-105987 and Craig H. Neilsen Foundation Senior Research Award (295319).

## DATA AVAILABILITY STATEMENT

The data that support the findings of this study are available from the corresponding author upon reasonable request.

## REFERENCES

1. van Middendorp JJ, Allison HC, Ahuja S, et al. Top ten research priorities for spinal cord injury: the methodology and results of a British priority setting partnership. Spinal Cord 2016;54(5):341–46. doi:10.1038/sc.2015.199 [PubMed: 26554273]
2. Simpson LA, Eng JJ, Hsieh JTC. Wolfe and the spinal cord injury rehabilitation evidence (SCIRE) research team DL. The health and life priorities of individuals with spinal cord injury: a systematic review. J Neurotrauma. 2012;29(8):1548–1555. doi:10.1089/neu.2011.2226 [PubMed: 22320160]
3. Anderson KD. Targeting recovery: priorities of the spinal cord-injured population. J Neurotrauma. 2004;21(10):1371–1383. doi:10.1089/neu.2004.21.1371 [PubMed: 15672628]

4. Ebert E Gastrointestinal involvement in spinal cord injury: a clinical perspective. J Gastrointestin Liver Dis. 2012;21(1):75–82. [PubMed: 22457863]
5. Sanders KM. A case for interstitial cells of Cajal as pacemakers and mediators of neurotransmission in the gastrointestinal tract. Gastroenterology. 1996;111(2):492–515. doi:10.1053/gast.1996.111.pm8690216 [PubMed: 8690216]
6. Iino S, Horiguchi K. Interstitial cells of cajal are involved in neuro-transmission in the gastrointestinal tract. Acta Histochem Cytochem. 2006;39(6):145–153. doi:10.1267/ahc.06023 [PubMed: 17327901]
7. Sanders KM, Koh SD, Ward SM. Organization and electrophysiology of interstitial cells of Cajal and smooth muscle cells in the gastrointestinal tract. Physiology of the Gastrointestinal Tract. Elsevier; 2012:511–556. doi:10.1016/B978-0-12-382026-6.00018-X
8. Green SA, Uy BR, Bronner ME. Ancient evolutionary origin of vertebrate enteric neurons from trunk-derived neural crest. Nature. 2017;544(7648):88–91. doi:10.1038/nature21679 [PubMed: 28321127]
9. Furness JB, Stebbing MJ. The first brain: species comparisons and evolutionary implications for the enteric and central nervous systems. Neurogastroenterol Motil. 2018;30(2):e13234. doi:10.1111/nmo.13234
10. Smith TK, Robertson WJ. Synchronous movements of the longitudinal and circular muscle during peristalsis in the isolated Guinea-pig distal colon. J Physiol. 1998;506(2):563–577. doi:10.1111/j.1469-7793.1998.563bw.x [PubMed: 9490879]
11. Torihashi S, Ward SM, Nishikawa S, Nishi K, Kobayashi S, Sanders KM. c-kit-dependent development of interstitial cells and electrical activity in the murine gastrointestinal tract. Cell Tissue Res. 1995;280(1):97–111. doi:10.1007/BF00304515 [PubMed: 7538451]
12. Kim YC, Koh SD, Sanders KM. Voltage-dependent inward currents of interstitial cells of Cajal from murine colon and small intestine. J Physiol. 2002;541(Pt 3):797–810. doi:10.1113/jphysiol.2002.018796 [PubMed: 12068041]
13. Zhu MH, Kim TW, Ro S, et al. A Ca(2+)-activated Cl(−) conductance in interstitial cells of Cajal linked to slow wave currents and pacemaker activity. J Physiol. 2009;587(Pt 20):4905–4918. doi:10.1113/jphysiol.2009.176206 [PubMed: 19703958]
14. den Braber-Ymker M, Lammens M, van Putten MJAM, Nagtegaal ID. The enteric nervous system and the musculature of the colon are altered in patients with spina bifida and spinal cord injury. Virchows Arch. 2017;470(2):175–184. doi:10.1007/s00428-016-2060-4 [PubMed: 28062917]
15. White AR, Holmes GM. Anatomical and functional changes to the colonic neuromuscular compartment after experimental spinal cord injury. J Neurotrauma. 2017;35(9):1079–1090. doi:10.1089/neu.2017.5369
16. White AR, Werner CM, Holmes GM. Diminished enteric neuro-muscular transmission in the distal colon following experimental spinal cord injury. Exp Neurol. 2020;331:113377. doi:10.1016/j.expneurol.2020.113377 [PubMed: 32526238]
17. Scheff SW, Rabchevsky AG, Fugaccia I, Main JA, Lumpp JE. Experimental modeling of spinal cord injury: characterization of a force-defined injury device. J Neurotrauma. 2003;20(2):179–193. doi:10.1089/08977150360547099 [PubMed: 12675971]
18. Tong M, Qualls-Creekmore E, Browning KN, Travagli RA, Holmes GM. Experimental spinal cord injury in rats diminishes vagally-mediated gastric responses to cholecystokinin-8s. Neurogastroenterol Motil. 2011;23(2):e69–e79. doi:10.1111/j.1365-2982.2010.01616.x [PubMed: 20950355]
19. Totoiu MO, Keirstead HS. Spinal cord injury is accompanied by chronic progressive demyelination. J Comp Neurol. 2005;486(4):373–383. doi:10.1002/cne.20517 [PubMed: 15846782]
20. Yu CS, Kim HC, Hong HK, et al. Evaluation of myenteric ganglion cells and interstitial cells of Cajal in patients with chronic idiopathic constipation. Int J Color Dis. 2002;17(4):253–258. doi:10.1007/s00384-001-0380-5
21. Bernardini N, Segnani C, Ippolito C, et al. Immunohistochemical analysis of myenteric ganglia and interstitial cells of Cajal in ulcerative colitis. J Cell Mol Med. 2012;16(2):318–327. doi:10.1111/j.1582-4934.2011.01298.x [PubMed: 21426484]

22. Gomez-Pinilla PJ, Gibbons SJ, Sarr MG, et al. Changes in interstitial cells of cajal with age in the human stomach and colon. Neurogastroenterol Motil. 2011;23(1):36–44. doi:10.1111/j.1365-2982.2010.01590.x [PubMed: 20723073]

23. Vanderwinden JM, Rumessen JJ, Liu H, Descamps D, Laet MD, Vanderhaeghen JJ. Interstitial cells of Cajal in human colon and in Hirschsprung's disease. Gastroenterology. 1996;111(4):901–910. doi:10.1016/S0016-5085(96)70057-4 [PubMed: 8831584]

24. Kulkarni S, Micci MA, Leser J, et al. Adult enteric nervous system in health is maintained by a dynamic balance between neuronal apoptosis and neurogenesis. Proc Natl Acad Sci U S A. 2017;114(18):E3709–E3718. doi:10.1073/pnas.1619406114 [PubMed: 28420791]

25. Huizinga JD, Zarate N, Farrugia G. Physiology, injury and recovery of interstitial cells of Cajal: basic and clinical science. Gastroenterology. 2009;137(5):1548–1556. doi:10.1053/j.gastro.2009.09.023 [PubMed: 19778538]

26. Ward SM, Burns AJ, Torihashi S, Sanders KM. Mutation of the proto-oncogene c-kit blocks development of interstitial cells and electrical rhythmicity in murine intestine. J Physiol. 1994;480(Pt 1):91–97. doi:10.1113/jphysiol.1994.sp020343 [PubMed: 7853230]

27. Rich A, Miller SM, Gibbons SJ, Malysz J, Szurszewski JH, Farrugia G. Local presentation of steel factor increases expression of c-kit immunoreactive interstitial cells of Cajal in culture. Am J Physiol Gastrointest Liver Physiol. 2003;284(2):G313–G320. doi:10.1152/ajpgi.00093.2002 [PubMed: 12388202]

28. Huizinga JD, Thuneberg L, Klüppel M, Malysz J, Mikkelsen HB, Bernstein A. W/kit gene required for interstitial cells of Cajal and for intestinal pacemaker activity. Nature. 1995;373(6512):347–349. doi:10.1038/373347a0 [PubMed: 7530333]

29. Maeda H, Yamagata A, Nishikawa S, et al. Requirement of c-kit for development of intestinal pacemaker system. Development. 1992;116(2):369–375. doi:10.1242/dev.116.2.369 [PubMed: 1283735]

30. Han J, Zhou YP, Jiang YZ, He YT, Mei F. Postnatal development of interstitial cells of Cajal in mouse colon in response to kit signal blockade with imatinib (Glivec). Acta Histochem. 2010;112(3):215–221. doi:10.1016/j.acthis.2010.02.003 [PubMed: 20199801]

31. Sanders KM, Ward SM. Kit mutants and gastrointestinal physiology. J Physiol. 2007;578(Pt 1):33–42. doi:10.1113/jphysiol.2006.122473 [PubMed: 17095561]

32. Iino S, Horiguchi K, Horiguchi S. c-kit-stem cell factor signal-independent development of interstitial cells of Cajal in murine small intestine. Cell Tissue Res. 2020;379(1):121–129. doi:10.1007/s00441-019-03120-9 [PubMed: 31741038]

33. Osada T, Watanabe M, Hasuo A, et al. Efficacy of the coadministration of granulocyte colony-stimulating factor and stem cell factor in the activation of intrinsic cells after spinal cord injury in mice. J Neurosurg Spine. 2010;13(4):516–523. doi:10.3171/2010.4.SPINE09973 [PubMed: 20887150]

34. Chio JCT, Xu KJ, Popovich P, David S, Fehlings MG. Neuroimmunological therapies for treating spinal cord injury: evidence and future perspectives. Exp Neurol. 2021;341:113704. doi:10.1016/j.expneurol.2021.113704 [PubMed: 33745920]

35. Kröncke KD, Fehsel K, Kolb-Bachofen V. Nitric oxide: cytotoxicity versus cytoprotection—how, why, when, and where? Nitric Oxide. 1997;1(2):107–120. doi:10.1006/niox.1997.0118 [PubMed: 9701050]

36. Laurent M, Lepoivre M, Tenu JP. Kinetic modelling of the nitric oxide gradient generated in vitro by adherent cells expressing inducible nitric oxide synthase. Biochem J. 1996;314(Pt 1):109–113. doi:10.1042/bj3140109 [PubMed: 8660270]

37. Choi KM, Gibbons SJ, Roeder JL, et al. Regulation of inter-stitial cells of Cajal in the mouse gastric body by neuronal nitric oxide. Neurogastroenterol Motil. 2007;19(7):585–595. doi:10.1111/j.1365-2982.2007.00936.x [PubMed: 17593140]

38. He CL, Soffer EE, Ferris CD, Walsh RM, Szurszewski JH, Farrugia G. Loss of interstitial cells of cajal and inhibitory innervation in insulin-dependent diabetes. Gastroenterology. 2001;121(2):427–434. doi:10.1053/gast.2001.26264 [PubMed: 11487552]

39. Kaji N, Horiguchi K, Iino S, et al. Nitric oxide-induced oxidative stress impairs pacemaker function of murine interstitial cells of Cajal during inflammation. Pharmacol Res. 2016;111:838–848. doi:10.1016/j.phrs.2016.07.030 [PubMed: 27468647]
40. Raybould HE, Glatzle J, Robin C, et al. Expression of 5-HT3 receptors by extrinsic duodenal afferents contribute to intestinal inhibition of gastric emptying. Am J Physiol Gastrointest Liver Physiol. 2003;284(3):G367–G372. doi:10.1152/ajpgi.00292.2001 [PubMed: 12409280]
41. Jin JG, Foxx-Orenstein AE, Grider JR. Propulsion in Guinea pig colon induced by 5-hydroxytryptamine (HT) via 5-HT4 and 5-HT3 receptors. J Pharmacol Exp Ther. 1999;288(1):93–97. [PubMed: 9862758]
42. Kadowaki M, Wade PR, Gershon MD. Participation of 5-HT3, 5-HT4, and nicotinic receptors in the peristaltic reflex of Guinea pig distal colon. Am J Phys. 1996;271(5 Pt 1):G849–G857. doi:10.1152/ajpgi.1996.271.5.G849
43. Liu MT, Kuan YH, Wang J, Hen R, Gershon MD. 5-HT4 receptor-mediated neuroprotection and neurogenesis in the enteric nervous system of adult mice. J Neurosci. 2009;29(31):9683–9699. doi:10.1523/JNEUROSCI.1145-09.2009 [PubMed: 19657021]
44. Heredia DJ, Dickson EJ, Bayguinov PO, Hennig GW, Smith TK. Localized release of serotonin (5-hydroxytryptamine) by a fecal pellet regulates migrating motor complexes in murine colon. Gastroenterology. 2009;136(4):1328–1338. doi:10.1053/j.gastro.2008.12.010 [PubMed: 19138686]
45. Wouters MM, Gibbons SJ, Roeder JL, et al. Exogenous serotonin regulates proliferation of interstitial cells of Cajal in mouse jejunum through 5-HT2B receptors. Gastroenterology. 2007;133(3):897–906. doi:10.1053/j.gastro.2007.06.017 [PubMed: 17854596]
46. Tharayil VS, Wouters MM, Stanich JE, et al. Lack of serotonin 5-HT2B receptor alters proliferation and network volume of interstitial cells of Cajal in vivo. Neurogastroenterol Motil. 2010;22(4):462–469, e109–110. doi:10.1111/j.1365-2982.2009.01435.x [PubMed: 19941613]
47. Liu M, Geddis MS, Wen Y, Setlik W, Gershon MD. Expression and function of 5-HT4 receptors in the mouse enteric nervous system. Am J Physiol Gastrointest Liver Physiol. 2005;289(6):G1148–G1163. doi:10.1152/ajpgi.00245.2005 [PubMed: 16037544]
48. Glatzle J, Sternini C, Robin C, et al. Expression of 5-HT3 receptors in the rat gastrointestinal tract. Gastroenterology. 2002;123(1):217–226. doi:10.1053/gast.2002.34245 [PubMed: 12105850]
49. Ordög T, Takayama I, Cheung WK, Ward SM, Sanders KM. Remodeling of networks of interstitial cells of Cajal in a murine model of diabetic gastroparesis. Diabetes. 2000;49(10):1731–1739. doi:10.2337/diabetes.49.10.17315 [PubMed: 11016458]
50. Grover M, Farrugia G, Lurken MS, et al. Cellular changes in diabetic and idiopathic gastroparesis. Gastroenterology. 2011;140(5):1575–1585. doi:10.1053/j.gastro.2011.01.046 [PubMed: 21300066]
51. Ippolito C, Segnani C, Errede M, et al. An integrated assessment of histopathological changes of the enteric neuromuscular compartment in experimental colitis. J Cell Mol Med. 2015;19(2):485–500. doi:10.1111/jcmm.12428 [PubMed: 25521239]
52. Kashyap P, Gomez-Pinilla PJ, Pozo MJ, et al. Immunoreactivity for Ano1 detects depletion of kit-positive interstitial cells of Cajal in patients with slow transit constipation. Neurogastroenterol Motil. 2011;23(8):760–765. doi:10.1111/j.1365-2982.2011.01729.x [PubMed: 21585622]
53. Huizinga JD, Hussain A, Chen JH. Interstitial cells of Cajal and human colon motility in health and disease. Am J Physiol Gastrointest Liver Physiol. 2021;321(5):G552–G575. doi:10.1152/ajpgi.00264.2021 [PubMed: 34612070]
54. Wei R, Parsons SP, Huizinga JD. Network properties of interstitial cells of Cajal affect intestinal pacemaker activity and motor patterns, according to a mathematical model of weakly coupled oscillators. Exp Physiol. 2017;102(3):329–346. doi:10.1113/EP086077 [PubMed: 28036151]
55. Hayashi Y, Toyomasu Y, Saravanaperumal SA, et al. Hyperglycemia increases interstitial cells of Cajal via MAPK1 and MAPK3 signaling to ETV1 and KIT, leading to rapid gastric emptying. Gastroenterology. 2017;153(2):521–535.e20. doi:10.1053/j.gastro.2017.04.020 [PubMed: 28438610]

56. Primeaux SD, Tong M, Holmes GM. Effects of chronic spinal cord injury on body weight and body composition in rats fed a standard chow diet. Am J Physiol Regul Integr Comp Physiol. 2007;293(3):R1102–R1109. doi:10.1152/ajpregu.00224.2007 [PubMed: 17634202]
57. Harris KK, Welch BA, Smith AM, Pride Y, Grayson BE. Altered chronic glycemic control in a clinically relevant model of rat thoracic spinal contusion. Biosci Rep. 2023;43(1):BSR20221699. doi:10.1042/BSR20221699 [PubMed: 36472154]
58. Pasricha PJ, Grover M, Yates KP, et al. Progress in gastroparesis—a narrative review of the work of the gastroparesis clinical research consortium. Clin Gastroenterol Hepatol. 2022;20(12):2684–2695.e3. doi:10.1016/j.cgh.2022.05.022 [PubMed: 35688353]
59. Dean AE, Reichardt F, Anakk S. Sex differences feed into nuclear receptor signaling along the digestive tract. Biochim Biophys Acta Mol basis Dis. 2021;1867(11):166211. doi:10.1016/j.bbadis.2021.166211 [PubMed: 34273530]
60. Gonzalez Z, Loganathan P, Sarosiek I, McCallum RW. Gender-related differences in gastroparesis. Am J Med Sci. 2020;360(5):474–483. doi:10.1016/j.amjms.2020.04.018 [PubMed: 32527595]
61. Kawano N, Koji T, Hishikawa Y, Murase K, Murata I, Kohno S. Identification and localization of estrogen receptor alpha-and beta-positive cells in adult male and female mouse intestine at various estrogen levels. Histochem Cell Biol. 2004;121(5):399–405. doi:10.1007/s00418-004-0644-6 [PubMed: 15138841]
62. Zielińska M, Fichna J, Bashashati M, et al. G protein-coupled estrogen receptor and estrogen receptor ligands regulate colonic motility and visceral pain. Neurogastroenterol Motil. 2017;29(7):e13025. doi:10.1111/nmo.13025
63. Liu JYH, Lin G, Fang M, Rudd JA. Localization of estrogen receptor ERα, ERβ and GPR30 on myenteric neurons of the gastrointestinal tract and their role in motility. Gen Comp Endocrinol. 2019;272:63–75. doi:10.1016/j.ygcen.2018.11.016 [PubMed: 30502347]
64. al -Shboul OA, Nazzal MS, Mustafa AG, et al. Estrogen relaxes gastric muscle cells via a nitric oxide- and cyclic guanosine monophosphate-ependent mechanism: a sex-associated differential effect. Exp Ther Med. 2018;16(3):1685–1692. doi:10.3892/etm.2018.6406 [PubMed: 30186388]
65. Brotfain E, Gruenbaum SE, Boyko M, Kutz R, Zlotnik A, Klein M. Neuroprotection by estrogen and progesterone in traumatic brain injury and spinal cord injury. Curr Neuropharmacol. 2016;14(6):641–653. doi:10.2174/1570159X14666160309123554 [PubMed: 26955967]
66. Sipski ML, Jackson AB, Gómez-Marín O, Estores I, Stein A. Effects of gender on neurologic and functional recovery after spinal cord injury. Arch Phys Med Rehabil. 2004;85(11):1826–1836. doi:10.1016/j.apmr.2004.04.031 [PubMed: 15520978]
67. Hubscher CH, Armstrong JE, Johnson JR. Effects of spinal cord injury on the rat estrous cycle. Brain Res. 2006;1100(1):118–124. doi:10.1016/j.brainres.2006.05.003 [PubMed: 16774748]
68. Bughi S, Shaw SJ, Mahmood G, Atkins RH, Szlachcic Y. Amenorrhea, pregnancy, and pregnancy outcomes in women following spinal cord injury: a retrospective cross-sectional study. Endocr Pract. 2008;14(4):437–441. doi:10.4158/EP.14.4.437 [PubMed: 18558596]
69. Kim SO, Song SH, Ahn KY, Kwon DD. Distribution of interstitial cells of Cajal in menopausal rat urinary bladder showing detrusor overactivity. Int Neurourol J. 2010;14(1):48–53. doi:10.5213/inj.2010.14.1.48 [PubMed: 21120176]
70. Bassotti G, Villanacci V, Bellomi A, et al. An assessment of enteric nervous system and estroprogestinic receptors in obstructed defecation associated with rectal intussusception. Neurogastroenterol Motil. 2012;24(3):e155–e161. doi:10.1111/j.1365-2982.2011.01850.x [PubMed: 22188470]

**Key Points**

- High-thoracic spinal cord injury (T3-SCI) induces proliferation of Interstitial Cells of Cajal located within the myenteric plexus.
- T3-SCI induces lengthening of primary arborizations for Interstitial Cells of Cajal within the myenteric plexus.
- Interstitial Cells of Cajal within the colonic smooth muscle layer do not exhibit significant changes after T3-SCI.
- There are sex differences in the rate of Interstitial Cells of Cajal remodeling after T3-SCI.

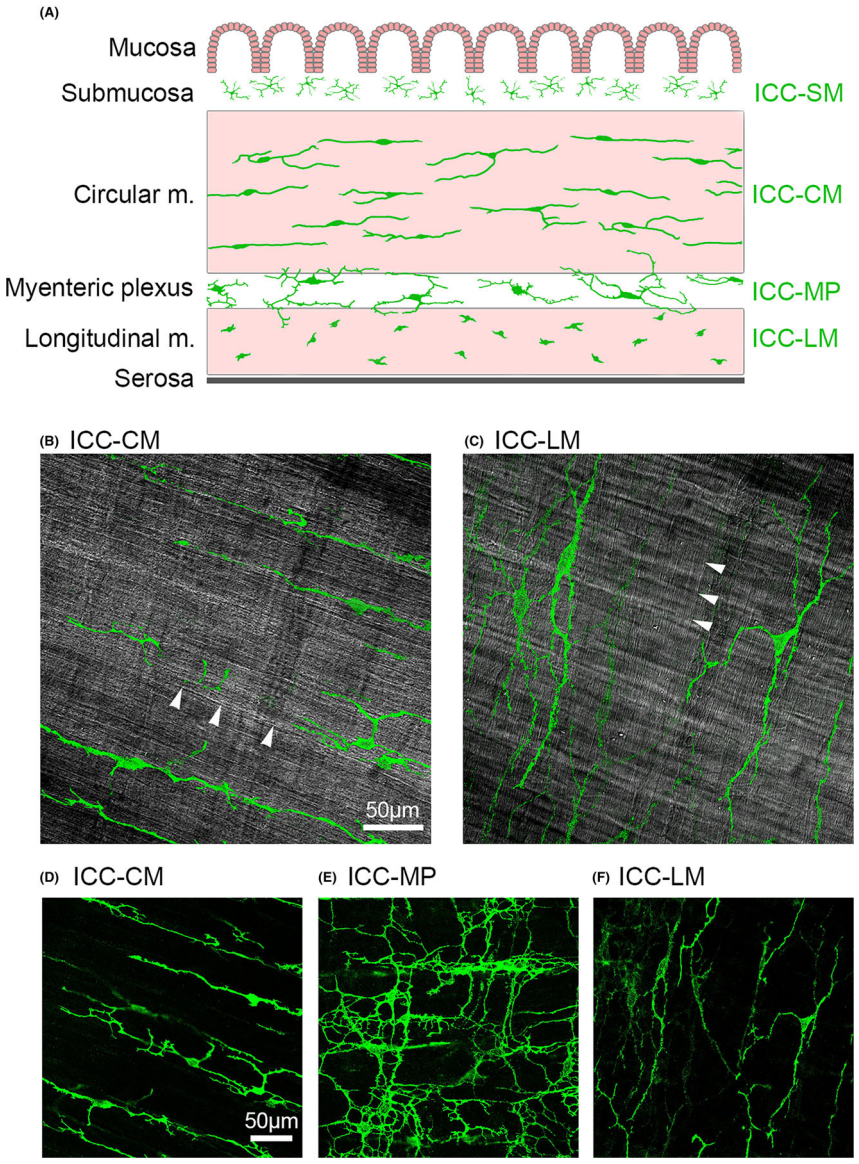


**FIGURE 1.**

(A) Schematic illustration of the layers of the distal colon smooth muscle (m.) with Interstitial Cells of Cajal (ICC) depicted in green. The mucosa and submucosa, including the multipolar ICC (ICC-SM) are removed for immunohistochemical processing. Intramuscular ICC are primarily bipolar and are distributed along the axis of the smooth muscle cells throughout circular muscle (ICC-CM) and perpendicularly-oriented longitudinal muscle (ICC-LM). The cells of the myenteric plexus (ICC-MP) are multipolar with numerous secondary and tertiary cytoplasmic branching. (B) Single z-stack image of DIC channel highlighting smooth muscle fiber orientation of the circular muscle at that plane of focus (white arrowheads) upon which intensity threshold-isolated ICC-CM visualized from the corresponding FITC channel have been superimposed to illustrate orientation. (C) Similar processing of the DIC channel to highlight the perpendicularly oriented longitudinal smooth muscle (arrowheads) and ICC-LM. Representative original c-Kit fluorescent image of

isolated (D) ICC-CM; (E) ICC-MP; and (F) ICC-LM as visualized for quantitative analysis. Images are 40×; calibration bar = 50 μm.

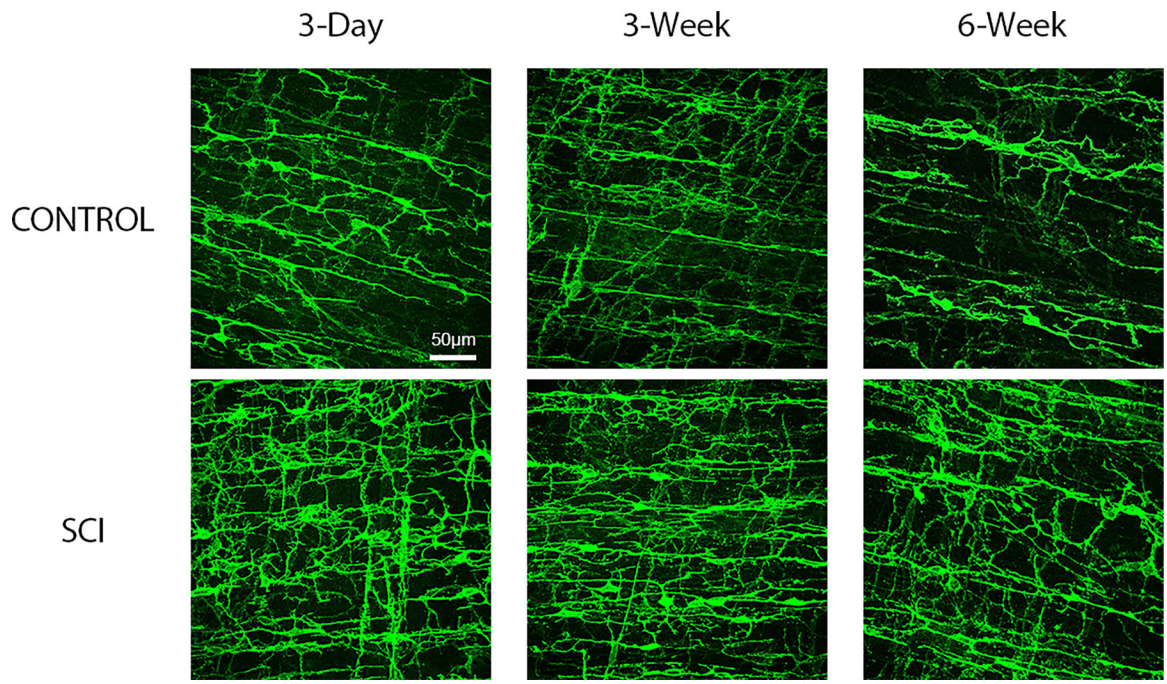


**FIGURE 2.**

Representative male rat surgical control and spinal cord injured (SCI) maximum projection confocal images of whole mounted distal colon processed for c-Kit immunofluorescent identification of myenteric and smooth muscle Interstitial Cells of Cajal (ICC). c-Kit immunofluorescence demonstrates an increase in pixel density beginning 3-days post-SCI compared to corresponding surgical controls, and this pattern is maintained at the 3 and 6-weeks time points. Images are 40× with scale bar = 50 μm.

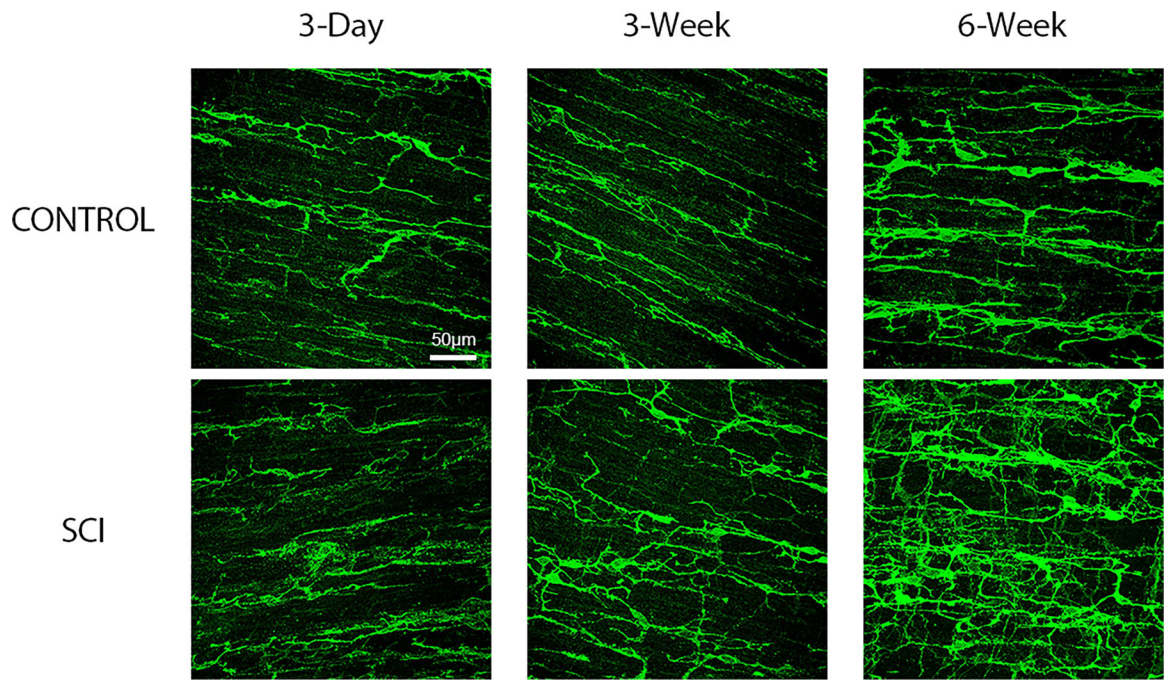


**FIGURE 3.**

Representative female rat surgical control and spinal cord injured (SCI) maximum projection confocal images of whole mounted distal colon processed for c-Kit immunofluorescent identification of myenteric and smooth muscle Interstitial Cells of Cajal (ICC). c-Kit immunofluorescence demonstrates an increase in pixel density beginning at 6-weeks post-SCI compared to corresponding surgical controls. Images are 40× with scale bar = 50 μm.

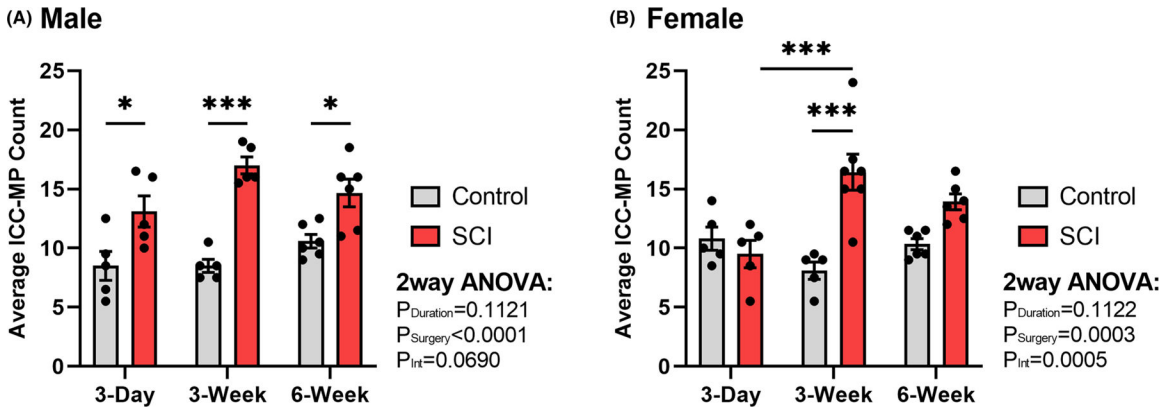


**FIGURE 4.**

Summary representation of surgical control and spinal cord injured (SCI) average number of myenteric plexus Interstitial Cells of Cajal (ICC-MP) within a randomly-selected field of view of uniform size. Graphs depict the average cell body count per animal in (A) male ($n$ = 32) and (B) female ($n$ = 34) rat distal colon. Compared to surgical controls, ICC-MP display the most notable increase at the 3-week time point following SCI for both sexes, although males demonstrate an increase at all time points postinjury. Values are expressed as mean ± SEM and considered significant at $p < 0.05$. All asterisks (*) are representative of Tukey's multiple comparisons test. Interaction values are representative of two-way ANOVA.

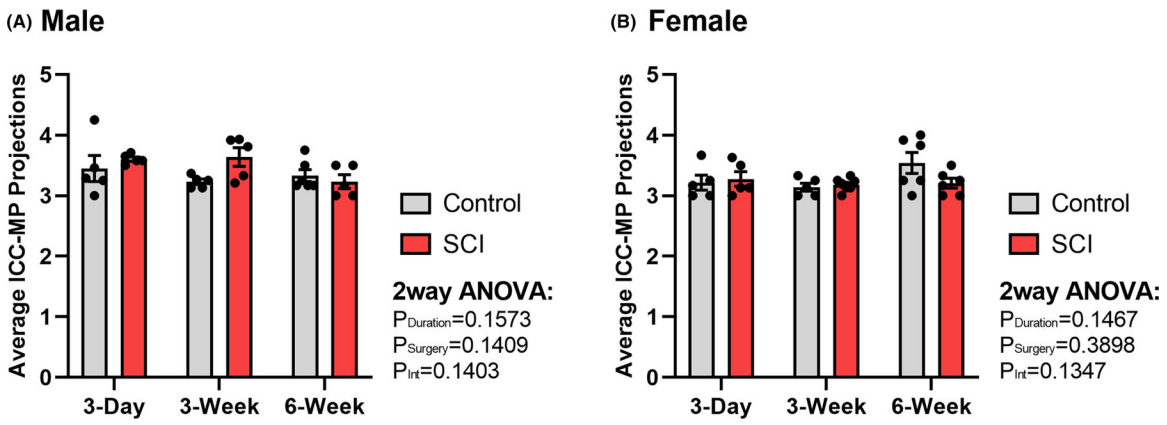


**FIGURE 5.**

Summary representation of surgical control and spinal cord injured (SCI) average number of primary (cytoplasmic) projections arising from individual myenteric Interstitial Cells of Cajal (ICC-MP) cell body per animal in (A) male ($n = 32$) and (B) female ($n = 34$) rat distal colon. No significant differences were identified between any groups as revealed by two-way ANOVA. Values are expressed as mean ± SEM. Interaction values are representative of two-way ANOVA.

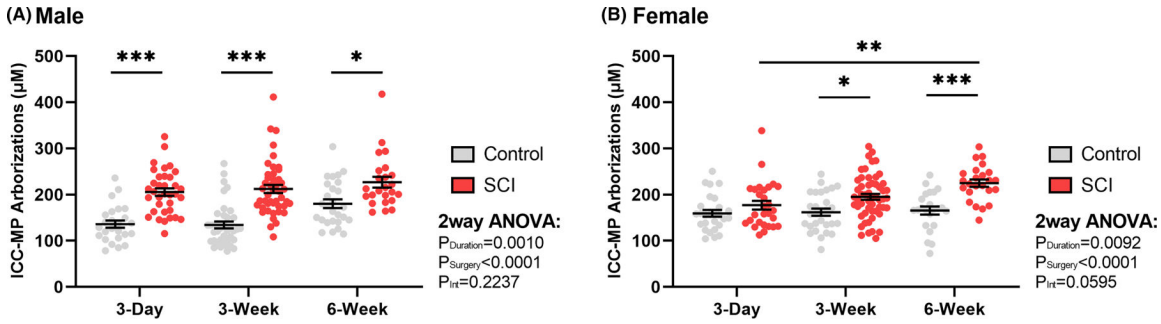


**FIGURE 6.**

Summary representation of surgical control and spinal cord injured (SCI) total primary arborization length per myenteric plexus Interstitial Cells of Cajal (ICC-MP) in (A) male ($n$ = 32) and (B) female ($n$ = 34) rat distal colon. While the number of primary arborizations do not increase following SCI, the cumulative primary arborizations increase in length for all male rat time points post-injury, and at chronic time points for females. Values are expressed as mean ± SEM and considered significant at $p < 0.05$. All asterisks (*) are representative of Tukey's multiple comparisons test. Interaction values are representative of two-way ANOVA.

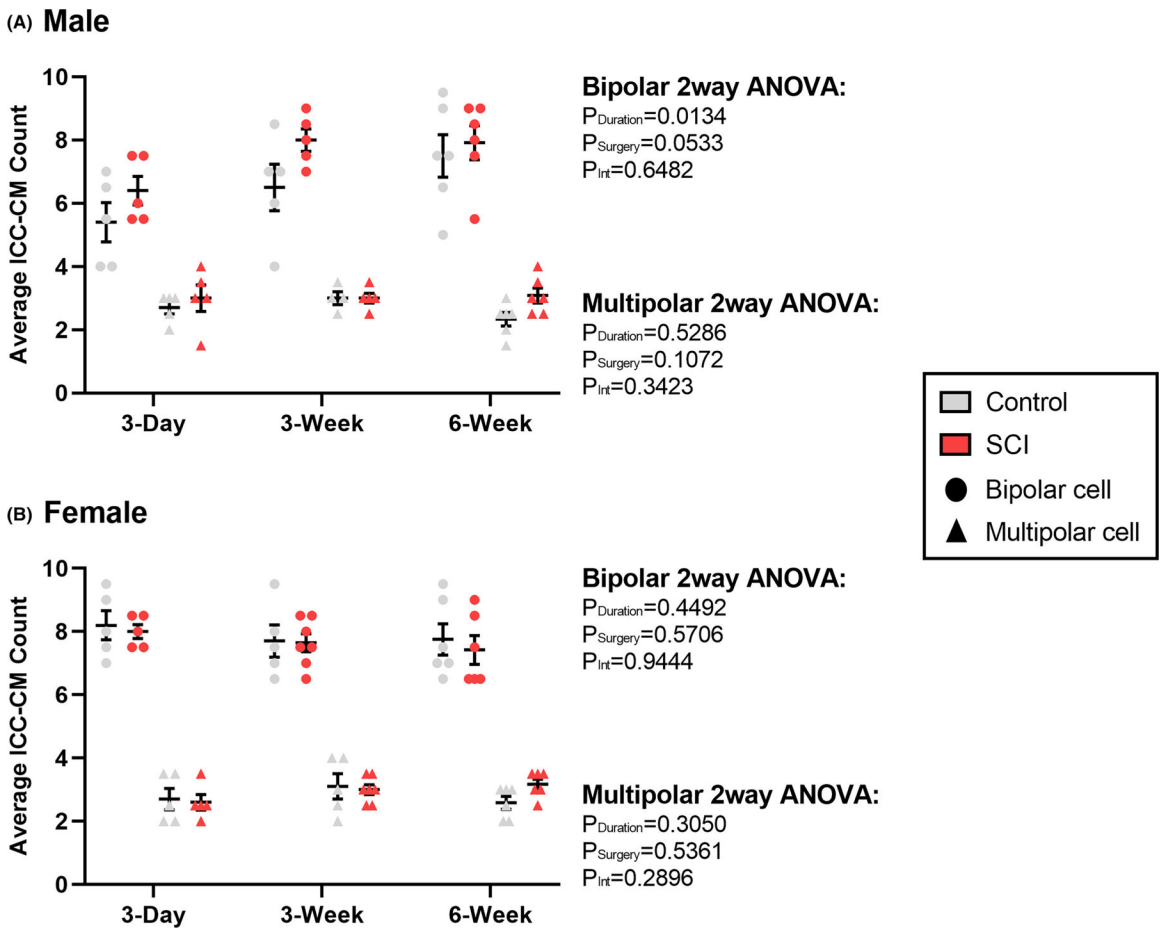


**FIGURE 7.**

Summary representation of surgical control and spinal cord injured (SCI) average number of circular muscle Interstitial Cells of Cajal (ICC-CM) within a randomly selected field of view of uniform size. Graphs depict the average cell body count per animal in (A) male ($n = 32$) and (B) female ($n = 34$) rat distal colon. Statistics were run independently for bipolar vs. multipolar cells due to known differences in their percentage of presentation. No significant differences were found between any groups. Values are expressed as mean ± SEM. Interaction values are representative of two-way ANOVA.

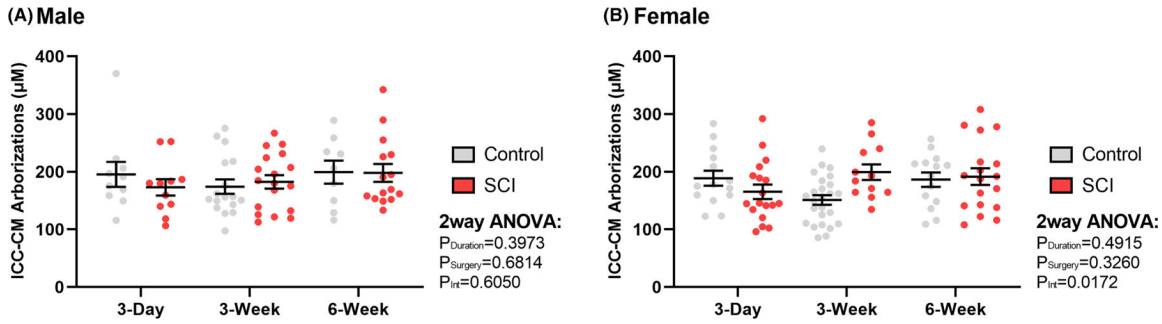


**FIGURE 8.**

Summary representation of surgical control and spinal cord injured (SCI) average number of circular muscle Interstitial Cells of Cajal (ICC-CM) per animal in (A) male ($n$ = 32) and (B) female ($n$ = 34) rat distal colon. Plotted points represent both bipolar and multipolar cells, as no significant relationship was found between morphology and arborization lengths. Values are expressed as mean ± SEM. Interaction values are representative of two-way ANOVA.